Engineering Journal issn: 0125-8281

Article

Strengthening of Shear-Critical RC Columns by High-Strength Steel-Rod Collars

Phawe Suit Theint[1,a], **Anat Ruangrassamee**[2,b,*], **and Qudeer Hussain**[2,c]

1 Department of Civil Engineering, Faculty of Engineering, Chulalongkorn University, Bangkok 10330, Thailand
2 Center of Excellence on Earthquake Engineering and Vibration, Department of Civil Engineering, Faculty of Engineering, Chulalongkorn University, Bangkok 10330, Thailand
E-mail: [a]phawesuit@gmail.com, [b]anat.r@chula.ac.th (Corresponding author), [c]ebbadat@hotmail.com

Abstract. This research investigates the strengthening of shear-dominated reinforced concrete (RC) square columns using the high-strength steel-rod collars, which enhance confinement by steel rods around the column perimeter. This method is less intrusive to the existing building with infilled walls because steel rods can penetrate through the walls with minimal openings (holes) at the location of collars. In this study, one control specimen and two specimens strengthened by steel-rod collars were tested. All specimens were subjected to lateral cyclic loading along with a constant axial load. The difference between the two strengthened specimens were the spacing of steel-rod collars mounted on the columns. The spacing of steel-rod collars was 200 mm in the column specimen SC-200, while the other strengthened specimen, SC-100 has a spacing of 100 mm. The unstrengthened column failed in shear while the strengthened columns failed in flexure. In addition, the strengthened specimens failed at the higher load and ductility. Comparing to the unstrengthened column, the lateral load capacity and ductility ratio of the column SC-200 increase by 18 % and 59%, respectively. While, the lateral load and ductility ratio of SC-100 increase by 16% and 69%, respectively. Furthermore, the finite element models of all column specimens are developed using the OpenSees program. The analysis results are found in a close agreement with the experimental results.

Keywords: Shear failure, RC column, shear strengthening, steel collars, OpenSees.

ENGINEERING JOURNAL Volume 24 Issue 3
Received 6 August 2019
Accepted 25 March 2020
Published 31 May 2020
Online at https://engj.org/
DOI:10.4186/ej.2020.24.3.107

DOI:10.4186/ej.2020.24.3.107

1. Introduction

During large earthquakes, several reinforced concrete (RC) members such as columns of buildings and bridges were damaged or completely collapsed (i.e., Northridge 1994, Kocaeli 1999 and Bam 2003) [1-2]. Some damage was attributed to inadequate shear strength or ductility of reinforced concrete (RC) columns. RC columns may have to be strengthened during their expected service life [3]. In the past, different strengthening schemes have been proposed and investigated to enhance the seismic performance of RC Columns [4]. Among them, the most conventional and wide accepted methods are mortar jacketing and concrete jacketing [5]. In concrete jacketing method, reinforcement embedded in the concrete is added around the column sections to increase strength, stiffness and ductility of RC columns. Extensive research efforts have been carried out in the past to investigate the lateral performance of RC columns with concrete jacketing [6-7]. Rodriguez and Park (1994) performed seismic load tests on reinforced concrete columns strengthened by concrete jacketing. Two arrangements of transverse reinforcement in the jacket were investigated. The as-built columns displayed low available ductility and significant degradation of strength during testing, whereas the jacketed columns behaved in a ductile manner with higher strength and much reduced strength degradation [7]. Recently, Bousias et al. (2007) investigated strength, stiffness, and cyclic deformation capacity of concrete jacketed members. Columns with plain vertical bars and no detailing for earthquake resistance are rehabilitated with shotcrete jackets connected to the old column through various means and subjected to cyclic uniaxial lateral loading up to ultimate conditions to investigate the effect of different means of connection at the interface on the effectiveness of the jacket. The test results indicate that the concrete jacketing is very useful to alter strength and stiffness of concrete jacketed members [8].

Although existing research proved the effectiveness of the concrete jacketing method, however, the concrete jacketing method is time-consuming and labor-intensive. To address these issues, use of externally bonded steel plates has been proposed and investigated by many researchers all around the world [9-11]. In this method, four straight or two L-shape steel plates are installed around the square or rectangular columns over required distance and connected together through welding and or bolts. The cement grout or other binder material are used to fill the gap between the steel plates and column. This method is referred to as the steel jacketing. Steel plate jacketing is proved very useful [12-13], however, this method involves the use of large steel plates and large amount of welding. To solve these issues, another method i.e., steel battens has been recently investigated to confine concrete by many researchers [14]. In this method, horizontal steel strips are used to confine concrete along with vertical steel angles at the column corners. The salient features of steel batten method are easy availability, light weight steel elements and easy installation at the site. Tarabia and Albakry 2014 performed laboratory tests and analytical investigation to study the response and efficiency of RC square columns externally strengthened by using steel angles and horizontal strips [14]. Authors reported that the use of steel angles and horizontal strips is very effective to enhance axial load carrying, strength and stiffness of the strengthened RC square columns. Although steel battens proved very useful to reduce the issue of the heavy steel plates, however, welding of the steel elements at the construction site required considerable time and accuracy. In addition, both methods i.e., steel plate jacketing and steel battens required binding material to fill the gap between the steel elements and concrete surface. Further, the installation process of both above mentioned methods for RC columns in existing building is very complex and required fully or partial removal of the adjacent walls.

Bernards et al., 1992 proposed a confining technique using steel-rod collars to enhance the strength, ductility and stiffness of RC columns [15]. The proposed steel-collars comprised four threaded steel rods, nuts and four corner elements made of steel angles. The advantages of steel-rod collars are low cost and minimum disturbance to the existing structures during the installation process. In addition, the installation method involves the use of nuts and does not require welding. Research findings indicate that steel-rod collars are effective to alter the shear strength of reinforced concrete columns [15]. It is important to note that the steel-rod collars experienced rupture during the tests and the abrupt drop of lateral load resistance was observed. Therefore, there is still the need to improve the detailing and installation method of the steel-collar method. In this research, the steel-collar method is improved by using high-strength steel rods to assure the ductile performance of strengthened columns. This method is less intrusive to the existing building with infilled walls because steel rods can penetrate through the walls with minimal openings (holes) at the location of collars as shown in Fig. 1. Both experimental and analytical studies are conducted to evaluate the strengthening efficiency of the proposed high-strength steel-rod collars.

2. Concept of Steel-Rod Collars

A typical view of the steel-rod collar system is shown in Fig. 1. Steel-rod collar system consists of threaded steel rods, nuts and corner elements made of steel angles.

In this study, a proper design procedure based on required shear strength is considered to determine the diameter of the threaded steel rods of the high-strength steel-rod collar. The corner elements in the steel-rod collar system comprises three pieces of steel angles as shown in Fig. 2. Steel angles were welded together to form a corner element. The bending moment due to tension in the steel rod was considered to determine the required sizes of the steel angle. The steel angle is L 65×65×8 mm. In addition, the middle portion of the steel rod was reduced in the diameter as shown in Fig. 3 to control the tension failure

within the region. A test was conducted to verify the failure mode as shown in Fig. 4. This was intended to ensure ductile behavior of the steel rod and to control the maximum tensile capacity of the steel rod.

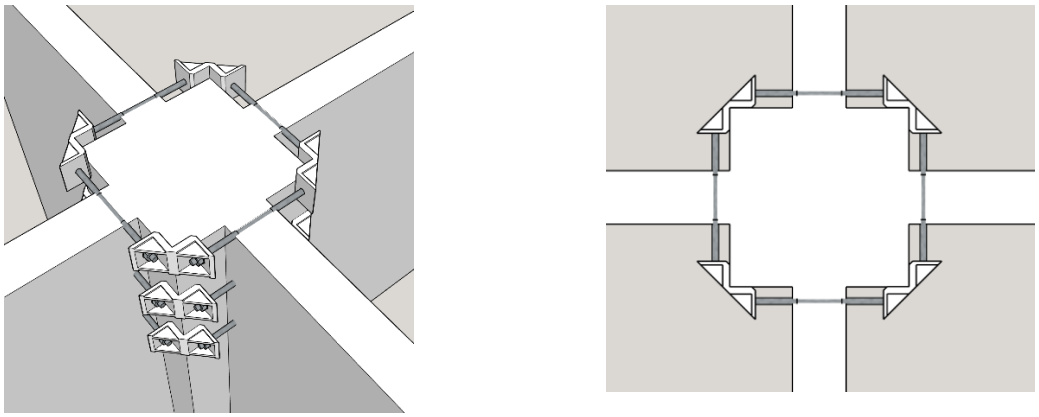

(a) Isometric view (b) Plan view

Fig. 1. Typical installation of the steel-rod collar system with masonry walls.

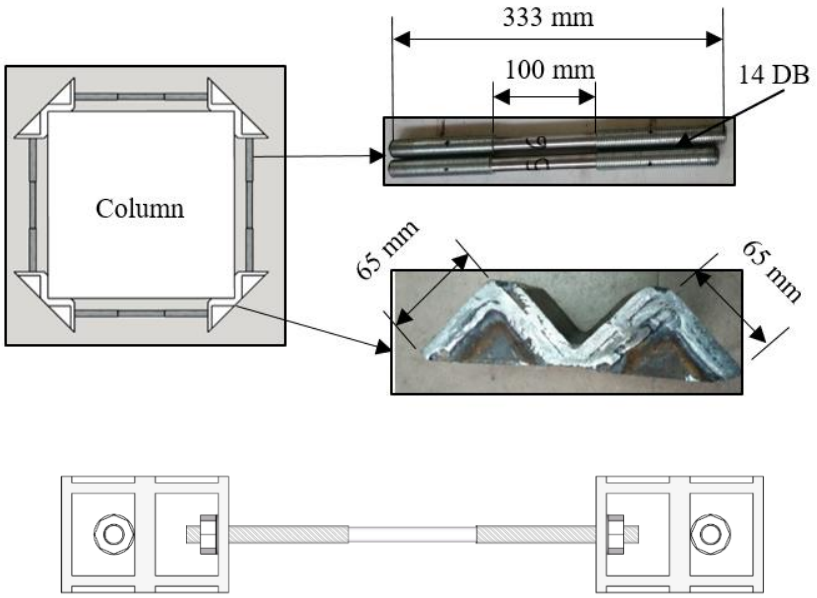

Fig. 2. Details of steel-rod collar system.

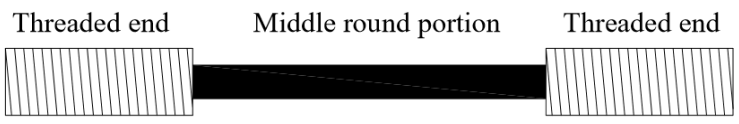

Fig. 3. Typical view of steel rod.

DOI:10.4186/ej.2020.24.3.107

Fig. 4. Tensile failure of steel rods.

3. Experimental Program

3.1. Specimens

In this study, three reinforced concrete columns with the same geometry and internal steel reinforcement were constructed and tested under lateral cyclic loading with a constant axial load. One RC column specimen was tested without any retrofitting method to serve as the control specimen. Whereas, remaining two columns SC-200 and SC -100 were strengthened with the high-strength steel-rod collar system. In columns SC-200 and SC-100, the steel rod collars were placed at 200 mm and 100 mm (center to center), respectively, as shown in Fig. 5. Fig. 6 show the dimensions in the section.

3.2. Details of RC Columns

The specimens were of the cantilever columns with oversized bases to be fixed to the strong floor. The column dimension was 400mm×400 mm. Sixteen vertical deformed bars (DB) with a nominal diameter of 20 mm were placed around the parameter of the section. The transverse steel ties were round bars (RB) of 9 mm in diameter with a vertical spacing of 300 mm for all RC columns. The reinforcing details of RC columns are shown in Fig. 7.

In this study, RC columns were designed as structural members having high stiffness and flexural capacity with low ductility and governed by shear failure. The design code ACI 318 [16] suggest that flexural capacity of reinforced concrete section can be calculated by

$$M = 0.85 f_c^{'} a b \left(\frac{h}{2} - \frac{b}{2}\right) + A s^{'} f_y^{'} \left(\frac{h}{2} - d_2\right) + A s f_y \left(d_1 - \frac{h}{2}\right) \quad (1)$$

where $f_c^{'}$ = compressive strength of concrete, a = depth of compression block, b = width of column section, h = height of column section, $A_s^{'}$ = steel area in compression, A_s = steel area in tension, d_2 = effective depth of compression steel, d_1 = effective depth of tension steel, f_y = yield strength of longitudinal steel bars in tension and f_y' = yield strength of longitudinal steel bars in compression.

Similarly, shear capacity of reinforced concrete columns can be calculated by following equations suggested by ACI 318 [16].

$$V = 0.166\sqrt{f_c^{'}}\left(1 + \frac{P}{13.8 b h}\right) b d_1 + \frac{A_v f_{yt} d_1}{s} \quad (2)$$

where P = Axial load capacity, A_v = area of transverse reinforcement, f_{yt} = yield strength of lateral reinforcement and s = spacing of lateral reinforcement.

By using above mentioned Eq. (1) and (2), calculated flexure capacity of control column is 5814 kN and calculated shear capacity of control column is 280 kN. The ratio of flexure to shear capacity is higher than 1.0, indicating that the control column is governed by shear failure.

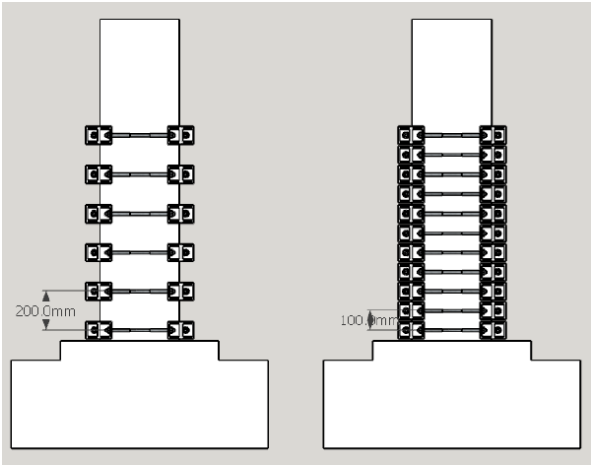

Fig. 5. Arrangement of steel-rod collars for SC-200 (left) and SC-100 (right).

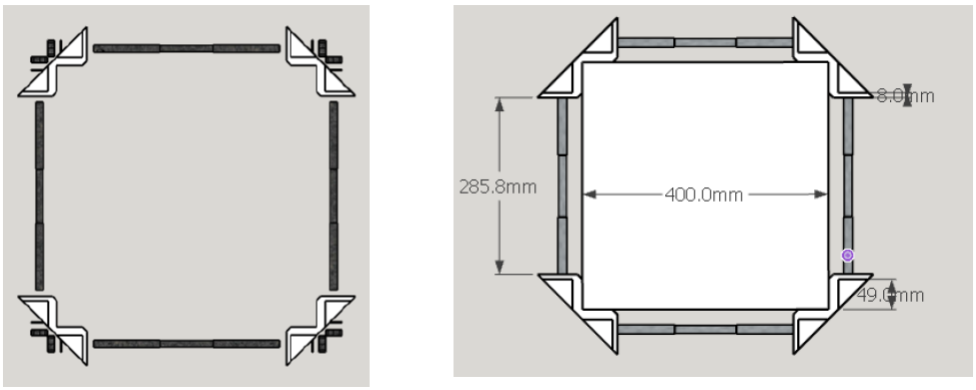

Fig. 6. Sectional arrangement of the steel-rod collars.

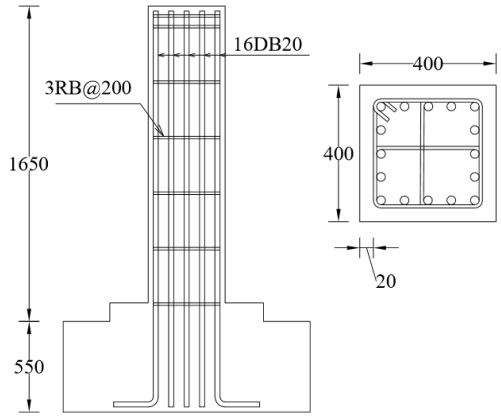

Fig. 7. Reinforcement details of RC columns (units: mm).

3.3. Material Properties

The ASTM C39 [17] standard was followed to determine the compressive strength of concrete. The average cylindrical compressive strength of concrete for test specimens was 31.5 MPa. The ASTM E8 [18] standard was followed to perform tensile tests of steel components. The longitudinal steel has a yield strength, f_y of 515 MPa and the transverse steel has a yield strength, f_{yt} of 299 MPa. The yield strength of the steel rod in the steel-rod collar, $f_{y\text{-}sc}$ is 442 MPa and the yield strength of the steel angle is 235 MPa.

3.4. Instrumentation

Strain gauges were installed on all specimens to record response during the test. Strain gauges were installed on longitudinal steel bars, transverse ties and steel rods. In longitudinal steel bars, stain gauges were installed between the transverse steel within the plastic hinge region as

shown in Fig. 8. The strain gauges were also installed on the transverse ties as shown in Fig. 9. At each level, three strain gauges were installed in the hoop tie and cross tie. In the steel-rod collars, strain gauges were installed as shown in Fig. 10 to monitor strains in the steel-rod collars during the test.

3.5. Loading Setup and Scheme

As in Fig. 11, the test specimens were subjected to displacement-controlled cyclic loading using the MTS 1500 kN hydraulic actuator connected to the reaction wall on one end and to the specimen on the other end. The load was applied at 1450 mm from the column base. A constant axial load of 0.16 $f_c' A_g$ was exerted by the manually-controlled hydraulic jack (where A_g is gross concrete area of column). The hydraulic jack was connected to sliding bearings which were supported by a steel frame as shown in the figure. When the specimen displaced horizontally, the hydraulic jack also moved horizontally along the column head to ensure that the force was applied vertically. Fig. 12 shows the photograph of the complete setup with all instrumentation.

The quasi-static lateral cyclic loading history under displacement control consisted of two consecutive cycles at each drift level as shown in Fig. 13. The lateral displacement ratio was increased by 0.25% until a drift ratio of 2% and then followed by an increasing step of 0.5%. The drift ratio is defined as the lateral displacement normalized by the height measured from the base to the loading point.

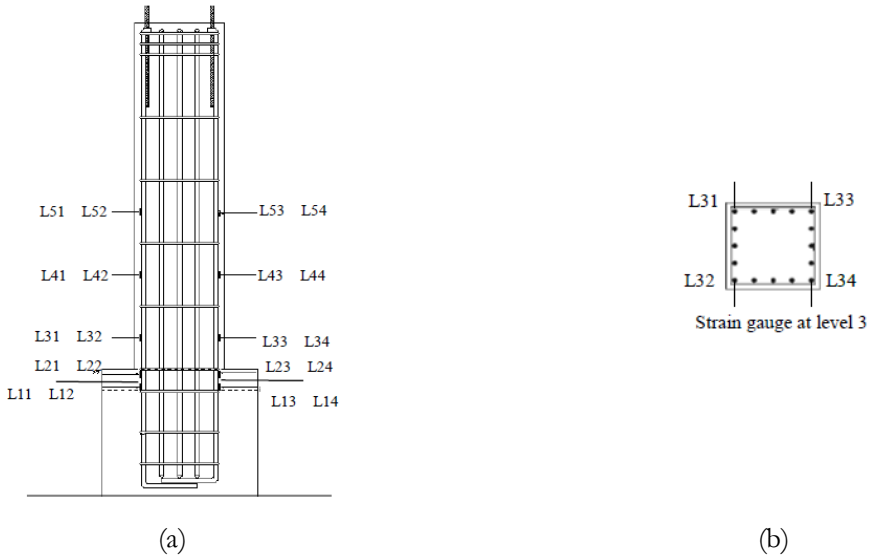

Fig. 8. Installation of strain gauges on vertical steel bars; a) elevation and b) section at level 3.

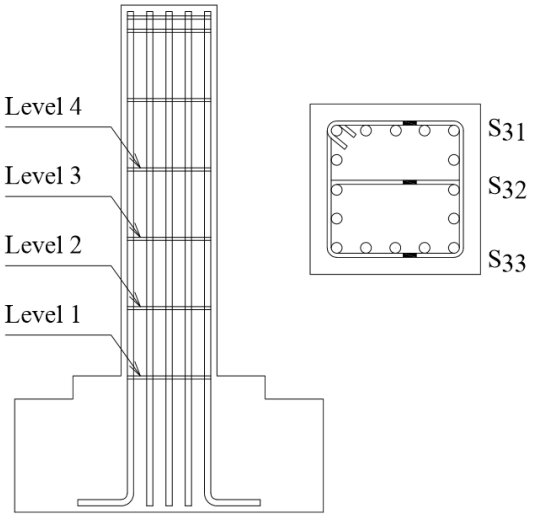

Fig. 9. Installation of strain gauges on ties a) elevation and b) section at level 3.

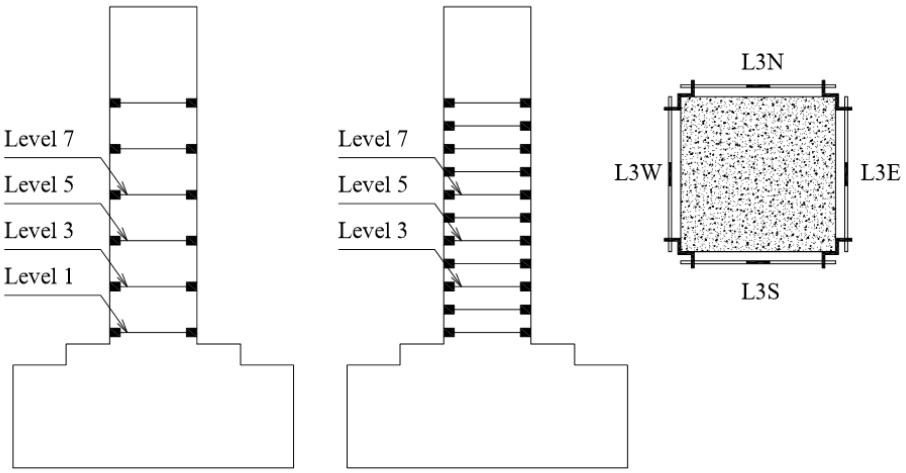

Fig. 10. Installation of strain gauges on steel-rod collars.

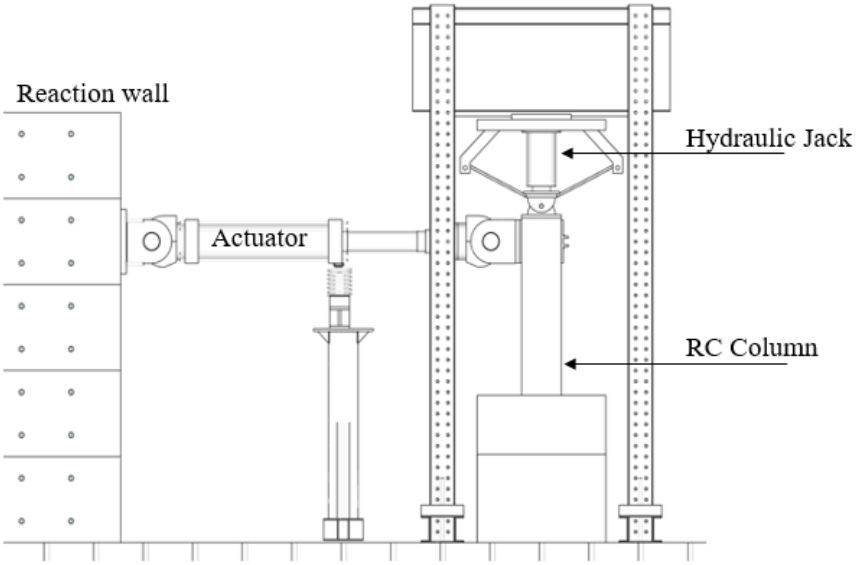

Fig. 11. Specimen connected to the actuator and hydraulic jack.

Fig. 12. Photograph of the complete test setup.

DOI:10.4186/ej.2020.24.3.107

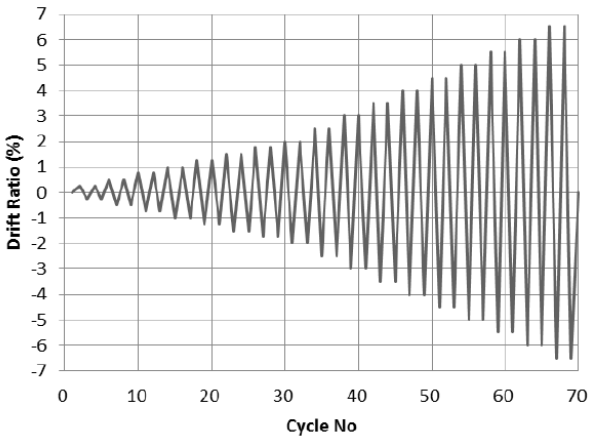

Fig. 13. Loading scheme.

4. Experimental Results

4.1. Damage Pattern

In un-strengthened RC column specimen, initial minor horizontal cracks (flexural cracks) appeared on the tension sides over the plastic hinge zone when the lateral displacement ratio was equal to 1.0%. With the further increase in the lateral drift ratio to 2.0%, initially observed cracks enlarged and extended further in the inclined direction. And crack widening and spalling of concrete was clearly observed. Both crack widening and spalling of concrete was increased with the further increase in the drift level. The final failure of the RC column was mainly due to large diagonal shear cracks spreading almost over the whole plastic hinge region when the lateral displacement was equal to a drift of 3.0%. This failure can be characterized as the brittle shear failure. Outward movement of transverse steel bars and buckling of the longitudinal steel bars was also evident as shown in Fig. 14. It can be noticed that the final failure of the control column is mainly due to the formation of the flexural-shear cracks, as a result of high tensile stress in the flexural reinforcement and shear-bond failure. Therefore, the final failure of the control columns is recognized as shear bond failure.

In the strengthened column SC-200, the initial horizontal flexural crack was also observed at a drift of 1.0%. With the further increase in the lateral drift level to 3.0%, initially observed cracks enlarged and extended further in the inclined direction. At this stage, several new cracks were also observed at both tension sides of the column. As the lateral drift reached 6.0%, crack widening and spalling of concrete was clearly observed. Both crack widening and spalling of concrete was increased with the further increase in displacement. The final failure of the column was mainly due to crushing of concrete at the base. The test was terminated at a lateral displacement of 6.50%. During the tests, it was noticed that steel rod collars at levels were remain tightened and undamaged. The effectiveness of the steel rod collars could be associated with the use of high strength threaded steel rods. In addition, ultimate strains in the threaded steel rods were found much lower than the yielding strains indicating the effectiveness of the proposed system to confine concrete. The behavior of the column SC-200 clearly indicates that the use of the steel-rod collar system is very effective to prevent concrete spalling and to delay the buckling of the longitudinal steel bars. Fig. 15 shows the damage of the column SC-200.

In the test of the column SC-100, the behavior is similar to the column SC-200 while the observed damage is less than the column SC-200 as shown in Fig. 16. The test was also terminated to a drift of 6.5%. The steel-rod collars at all levels remained undamaged during the whole test and the column also failed in the flexural mode.

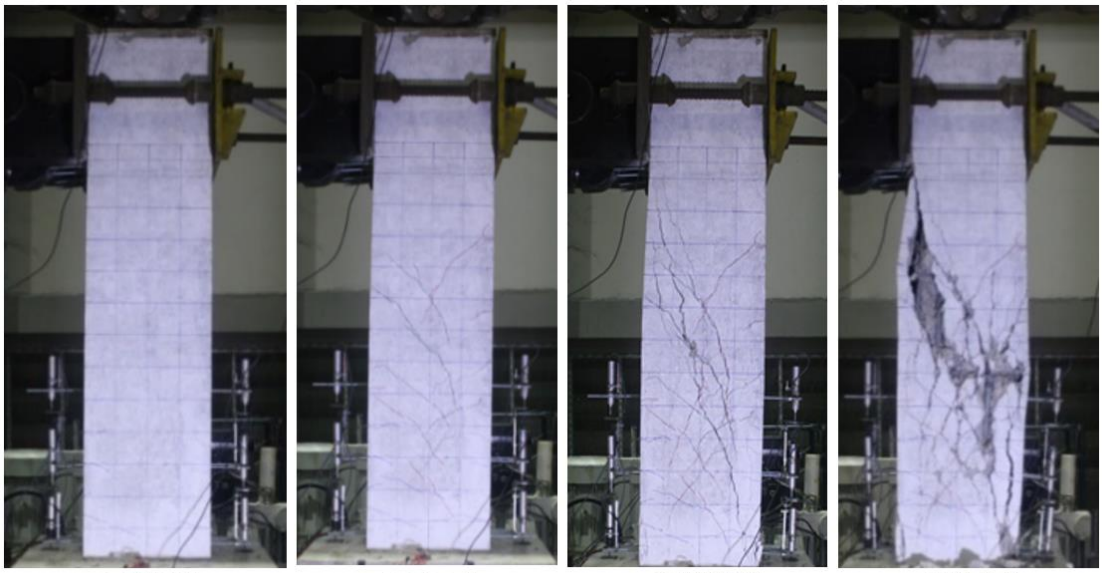

Fig. 14. Damage pattern of the control column.

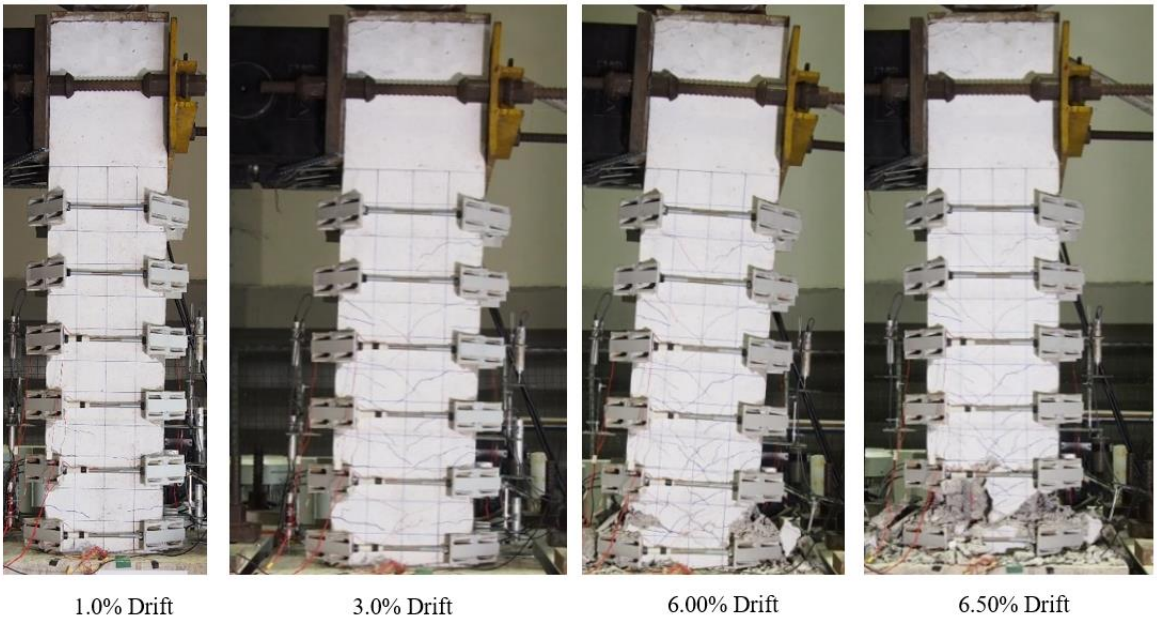

Fig. 15. Damage pattern of the column SC-200.

DOI:10.4186/ej.2020.24.3.107

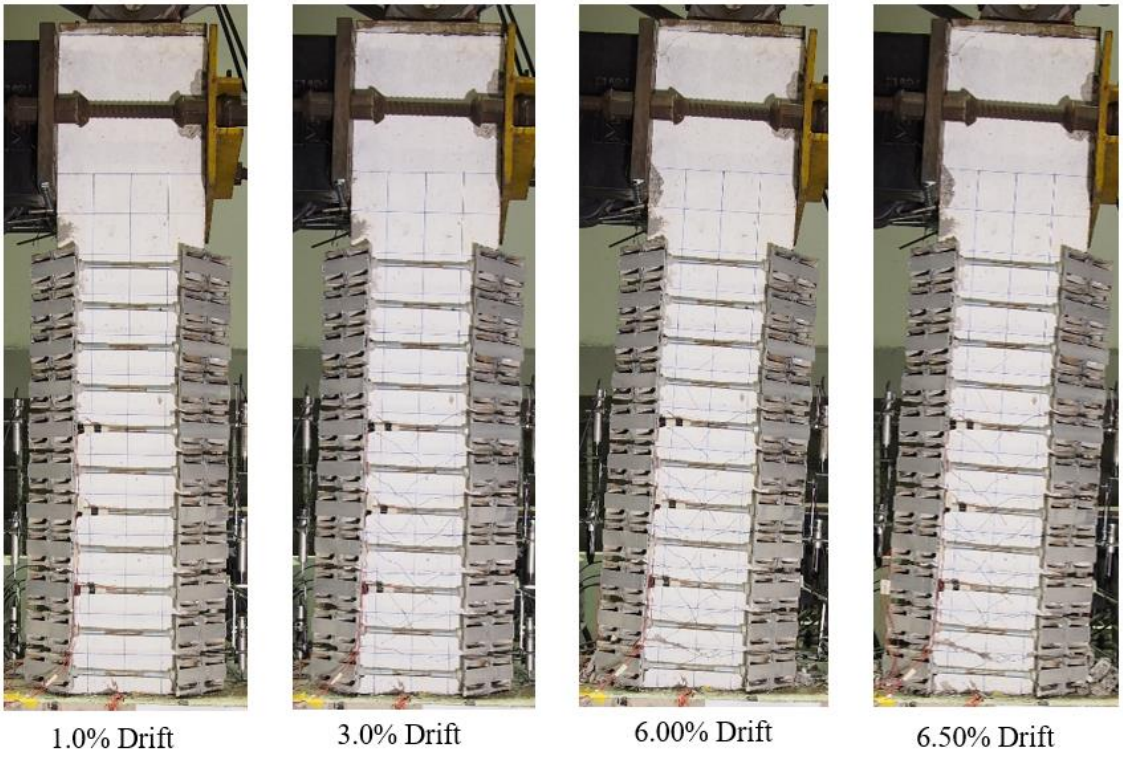

Fig. 16. Damage pattern of the column SC-100.

4.2. Load vs Displacement Relations

The load versus displacement relations for all three specimens are shown in Figs. 17-19. The envelop curves are compared in Fig. 20. It is evident from the figures that the hysteretic behavior of the columns strengthened by steel-rod collars (SC-200 and SC100) are significantly improved for each loading cycle when compared to the control column. The column SC100 has a slightly higher capacity and ductility than the column SC-200.

Table 1 summarizes the test results in terms of the maximum lateral load, drift level at 80% of peak load, yielding displacement, ultimate displacement, and displacement ductility. The yielding point was defined by the method proposed by Sezen and Moehle 2004 [19]. The lateral load capacity and ductility ratio of the column SC-200 increase by 18 % and 59%, respectively as compared to the column CC. While, the lateral load and ductility ratio of SC-100 increase by 16% and 69%, respectively.

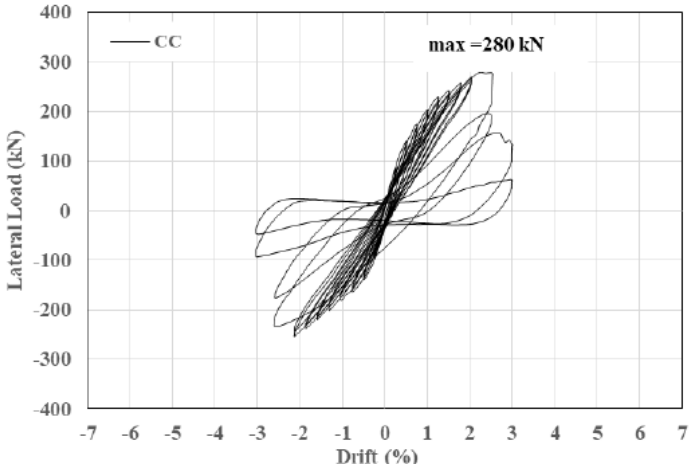

Fig. 17. Experimental lateral load vs. displacement curve of control column.

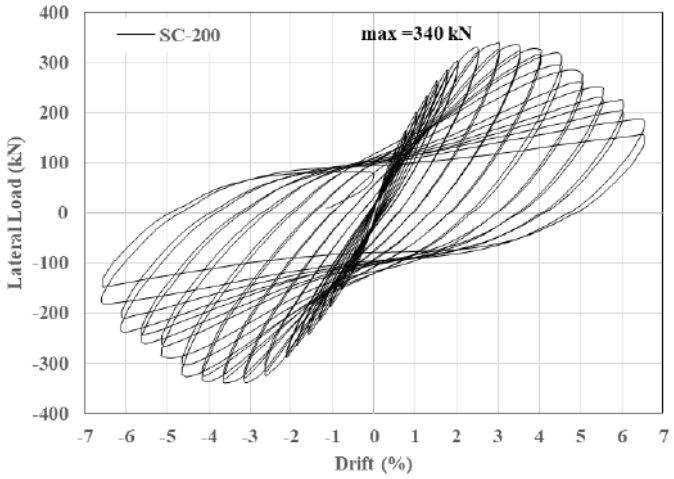

Fig. 18. Experimental lateral load vs. displacement curve of column SC-200.

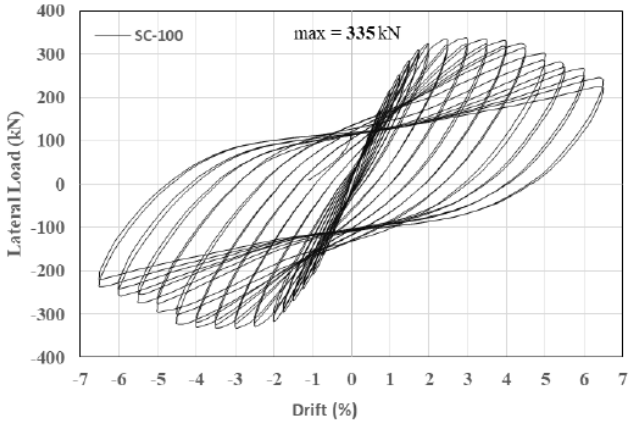

Fig. 19. Experimental lateral load vs. displacement curve of column SC-100.

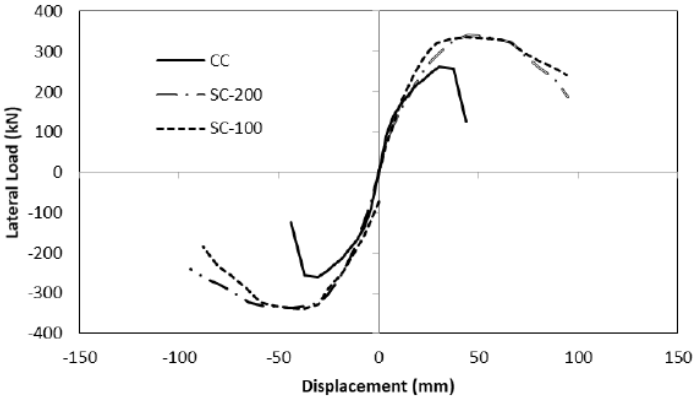

Fig. 20. Envelop curves of all columns.

DOI:10.4186/ej.2020.24.3.107

Table 1. Summary of key test results.

Test Columns	CC	SC-200	SC-100
Maximum lateral load (kN)	280	340	335
Drift at 80% of peak load (%)	2.7	5.4	5.8
Ultimate displacement, Δ_u(mm)	40	78	84.5
Yield displacement, Δ_y(mm)	37	29	24
Displacement Ductility, μ	1.1	2.7	3.5

4.3. Accumulated Energy Dissipation

To evaluate the effectiveness of strengthening by the steel-rod collar system, the comparison of energy dissipation is presented in Fig. 21. In case of the control (CC) column, lower energy dissipation was recorded. When the columns are strengthened by the steel-rod collar system, the total energy dissipation was greatly increased.

4.4. Strains in Longitudinal Steel Bars

Fig. 22 shows strains observed in longitudinal steel bars at the level 3. It is evident from figures that steel-rod collars are effective to stabilize the hysteretic behavior in the longitudinal steel bars because the premature shear failure did not occur in the strengthened columns. In case of strengthened columns, the longitudinal steel bars could undergo large strain levels even after yielding as shown in the figure.

4.5. Strains in Transverse Reinforcement

High strain values in steel ties were observed around the damaged zone. The strain in the transverse steels is presented in Fig. 23. It can be seen that steel-rod collars are very effective to delay yielding of steel ties. In case of the control column, the yielding of steel bars was observed at the final drift. On the other hand, in case of the column SC-200, yielding of steel ties was not observed at the peak lateral load. When the spacing of steel-rod collars was reduced as in the column SC-100, very low strain values were observed in the steel ties as shown in the figure. This is the clear indication that the steel rod collar system is effective to provide shear reinforcement to the shear deficient RC columns.

4.6. Strains in Steel-Rod Collars

In order to clearly understand the behavior of the steel-rod collar system, strain gauges were installed on the steel-rod collars. The strain values are shown in Fig. 24. It can be seen that ultimate strains in the steel rods were lower than the yielding strain and the steel-rod collars remained undamaged till the drop in the lateral load carrying capacity of the columns. This clearly shows the benefit of using the high-strength steel rod. In case of the column SC-200, the observed ultimate strain values in the steel-rod collars were relatively close to the yielding strain. When the spacing of steel-rod collars was reduced as in the column SC-100, there was a considerable reduction in the ultimate strain in the steel rod as seen in Fig. 24b.

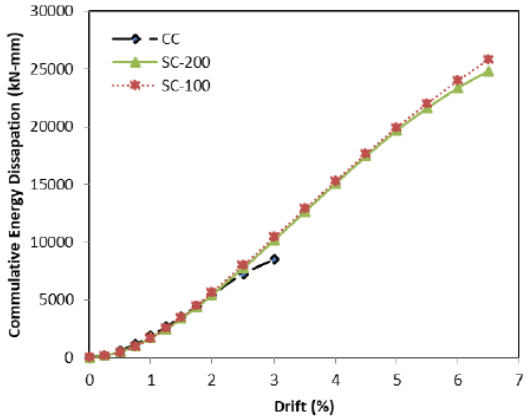

Fig. 21. Energy dissipation curves of specimens CC, SC-200 and SC-100.

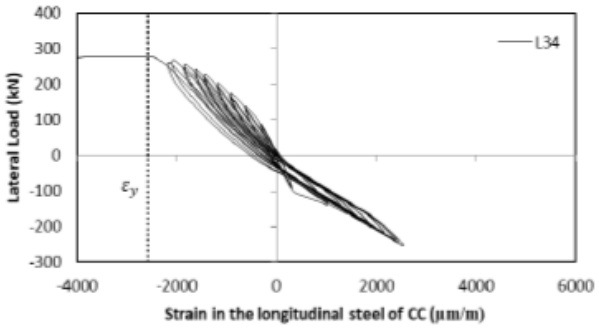

(a) Control Column

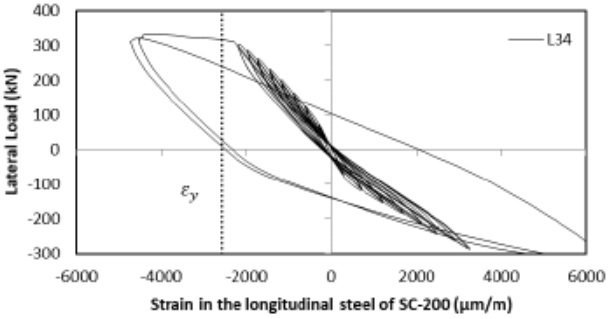

(b) Column SC-200

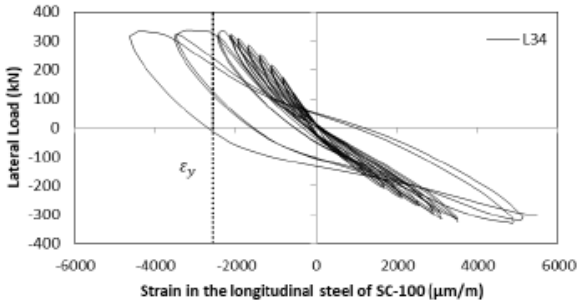

(c) Column SC-100

Fig. 22. Strain in longitudinal steel bars.

DOI:10.4186/ej.2020.24.3.107

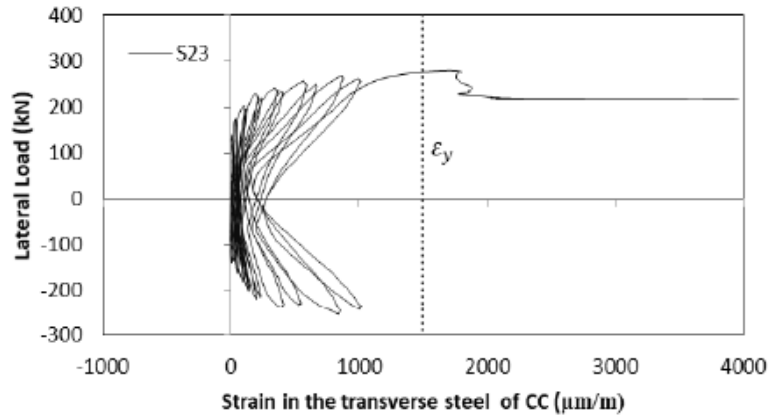

a) Control Column

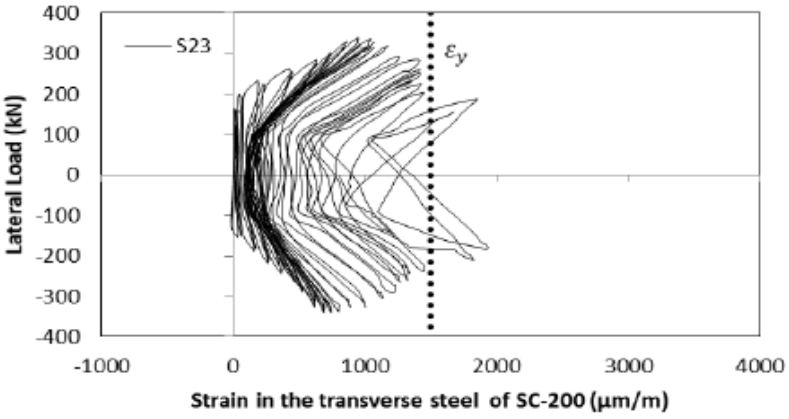

(b) Column SC-200

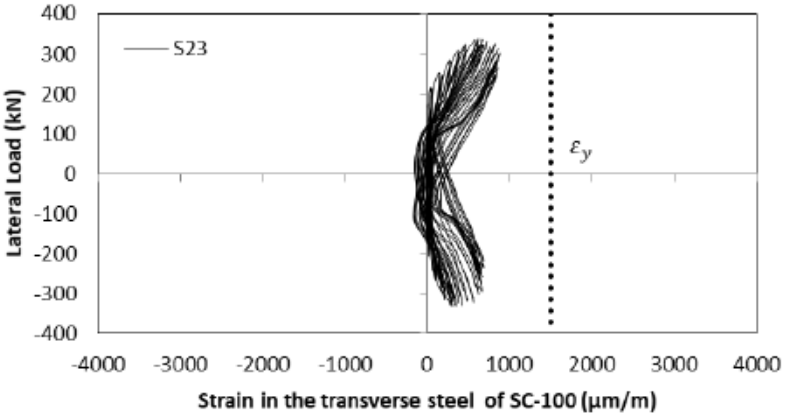

(c) Column SC-100

Fig. 23. Strain in transverse steel bars.

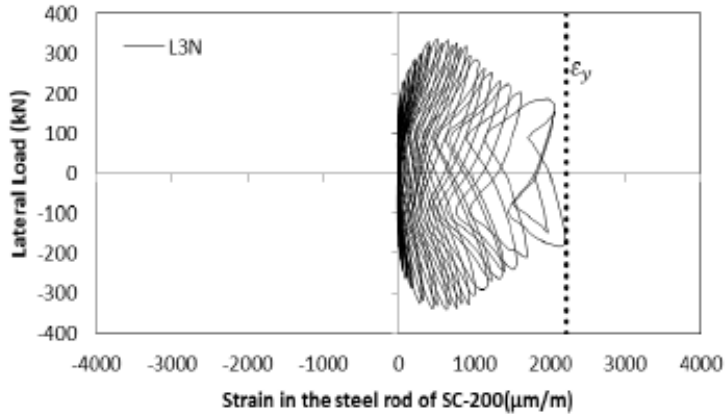

(a) Column SC-200

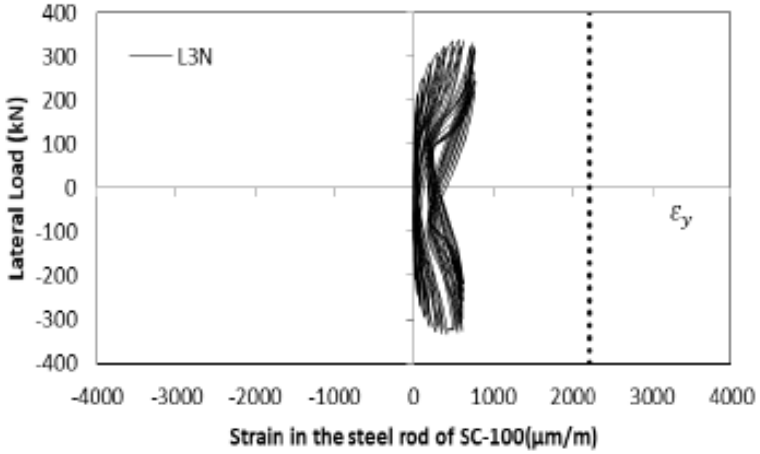

(b) RC Column SC-100

Fig. 24. Strain in steel-rod collars.

4.7. Shear Strength of Strengthened Columns

Many researchers had studied the theoretical stress strain model for the confined concrete and the confinement effect of the rectangular hoop with cross ties. Mander et al. [20] also studied the theoretical stress strain model for confined concrete and the confinement effectiveness for the rectangular concrete sections confined by rectangular hoop with cross ties. In this study, the concept of the theoretical model for confinement of concrete proposed by Mander et al. for rectangular hoops was applied in calculating the confinement effect produced by external steel-rod collars. The passive confinement of the column concrete was externally developed by the steel-rod collars. If a uniform tensile force is assumed to develop in the steel-rod collars, then the average confining pressure along both x-and y-directions (σ_x and σ_y, respectively) of a column section can be determined from the equilibrium and it can be expressed as follows:

$$\sigma_x = \frac{2A_v f_{yt}}{b_y s} \tag{3}$$

$$\sigma_y = \frac{2A_v f_{yt}}{b_x s} \tag{4}$$

This concept will be applied to calculate the contribution of the shear strength carried by the additional shear reinforcement from the steel-rod collars. Using the effective concrete area $0.8A_g$. Then the equation becomes

$$\begin{aligned} V_{sc} &= \left(\frac{2A_v f_{yt}}{b_y s} \times 0.8A_g\right) \\ &= \left(\frac{2A_v f_{yt}}{b_y s} \times b_y d_1\right) \\ &= \frac{2A_{st,sc} f_{y,sc}\, d_1}{s_{sc}} \text{ (MPa)} \end{aligned} \tag{5}$$

where, $A_{st,sc}$ = the area of steel-rod collars; A_v = area of transverse steel; $f_{y,sc}$ = the yield strength of steel-rod collars; s_{sc} = the spacing of the steel-rod collars; b_y = the width of the section in y direction; and bx = width of the section in x direction.

Aboutaha et al. [12] studied the rehabilitation of shear critical concrete columns by use of rectangular steel jackets and a simple model was developed to predict the shear

strength of jacketed columns and to determine the required thickness of the jacket. According to the previous study, the shear strength of the strengthened columns was determined by adding the shear strength of the jackets to the shear strength of the un-strengthened column. Therefore, to estimate the lateral shear strength capacity of the columns strengthened by steel-rod collars, the additional shear strength contribution of the steel-rod collars was added to the nominal shear strength of the un-strengthened specimen CC as follows:

$$V_n = V_c + V_s + V_{sc} \tag{6}$$

$$V_n = 0.166\sqrt{f'_c}\left(1+\frac{P}{13.8A_g}\right)bd_1 + \frac{A_S f_y d_1}{s} + V_{sc}\ (\text{MPa}) \tag{7}$$

$$V_n = 0.166\sqrt{f'_c}\left(1+\frac{P}{13.8A_g}\right)bd_1 + \frac{A_S f_y d_1}{s} + \frac{2A_{st,sc} f_{y,sc} d_1}{s_{sc}}\ (\text{MPa}) \tag{8}$$

According to the experimental test results, the maximum strengths of the specimens CC, SC-200 and SC100 were 280 kN, 335 kN and 340 kN respectively. The ratio of the measured capacity to calculated shear strength ratio for CC column was 1.12. After strengthening the columns, the lateral capacities of SC-200 and SC-100 were increased. The ratios of the measured capacity to calculated shear strength of SC-200 and SC-100 were 0.8 and 0.6, respectively. The estimated shear strength of proposed shear strength model is conservative because all steel-rod collars did not reach the yield strength. However, the strength in the steel-rod collars is considered at the yield strength in the calculation of shear force carried by steel-rod collars. Since the proposed equation is conservative, it can be used as a simplified shear strength equation for columns strengthened by steel-rod collars.

5. Numerical Analysis

The OpenSees program was used to model the test specimens in order to capture their behaviors [21]. The following sections explain the details of the models used in this study.

5.1. Model of Columns

The control column was the shear critical column, therefore, the beam column model with a shear spring was adopted to capture the shear failure of the column. Three different elements such as a fiber element, the rotational slip spring element and shear spring element were used to model the shear critical column in OpenSees. To capture the degradation in the shear strength, the shear spring with the rotational slip spring was used at the column base. The force-based fiber element was used to model the flexural behavior of the column. The numerical model of the control column is illustrated in Fig. 25.

The strengthened columns were modelled as illustrated in Fig. 26. Since the strengthened columns had sufficient shear reinforcement, the flexural behavior was dominant in the columns. So, the shear spring was not included in the model. The lumped plastic models have been found effective to model flexural columns [22-24]. The nonlinear response concentrates at the plastic hinge region (Lp) as shown in the figure. The properties of each components are explained in the following sections.

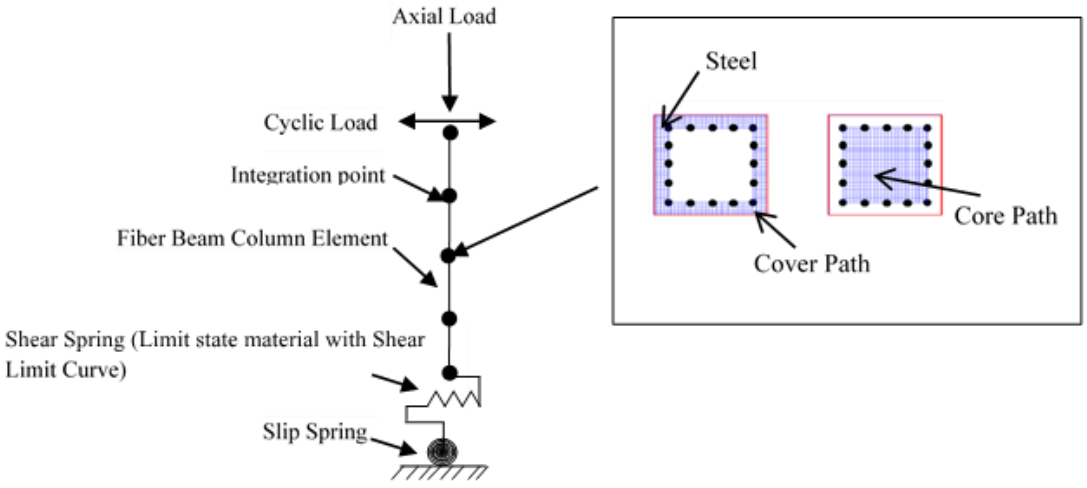

Fig. 25. Numerical model for the control column.

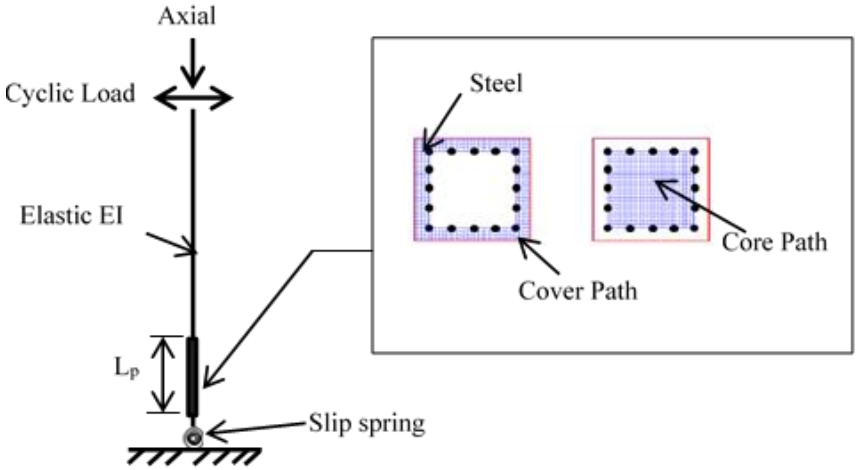

Fig. 26. Model of strengthened column.

5.2. Material Models

5.2.1. Unconfined concrete

The unconfined concrete fiber was assigned using the stress-strain behavior of concrete proposed by Kent and Park, 1971 [25]. The Concrete01 material model in OpenSees was used to represent the Kant and Park material model. Table 2 summarizes the properties used in the model.

5.2.2. Confined concrete

The material model proposed by Mander et al. [20] was adopted to represent the confined concrete. The Concrete02 material model was used to represent the Mander et al. model in OpenSees. The effective confining stress for the square column section is calculated as

$$f_l = k_e \rho_x f_y ;\ f_l = k_e \rho_y f_y \tag{9}$$

$$\rho_x = \frac{nA_v}{sb_c},\ \rho_y = \frac{nA_v}{sd_c} \tag{10}$$

$$k_e = \frac{\left(1-\sum_{i=1}^{n}\frac{(w_i)^2}{6b_c d_c}\right)\left(1-\frac{s-\phi}{2b_c}\right)\left(1-\frac{s-\phi}{2\mathrm{d}_c}\right)}{1-\rho_{cc}};\qquad \rho_{cc} = \frac{nA_s}{b_c d_c} \tag{11}$$

where k_e = confinement effectiveness coefficient; ϱ_x , ϱ_y = confining steel volumetric ratio in each direction; w_i = clear distance between longitudinal bars; c = clear cover; b_c = horizontal distance between hoops; d_c = vertical distance between hoops; ϱ_{cc} = ratio of longitudinal reinforcements to the area of core section; A_s = longitudinal reinforcement areas; n = number of steel bars; Ø = diameter of transverse reinforcement.

For the strengthened columns with steel-rod collars, the steel-rod collars provide the confining effect to the concrete. The confinement model for strengthened columns by [26) and [27] was adopted to calculate the confinement effectiveness coefficient (k_e) and confining steel volumetric ratio (ϱ_x, ϱ_y). The conceptual model for confined concrete with steel-rod collars is shown in Fig. 27.

The yield strength of steel-rod collars in the strengthened section has to be assigned in place of steel yield strength in Eq. (9) and the confining steel volumetric ratio of the steel-rod collars is calculated as in Eq. (12).

$$\rho_x = \frac{nA_{v,sc}}{sb},\ \rho_y = \frac{nA_{v,sc}}{sd} \tag{12}$$

Then, the confinement effectiveness coefficient (k_e), confining steel volumetric ratio for hoops and steel-rod collars (ϱ_x , ϱ_y) are described in the following equations:

$$k_e = \left(1-\frac{s-\phi_{sc}}{2b}\right)\left(1-\frac{s-\phi_{sc}}{2h}\right) \tag{13}$$

$$\rho_x = \frac{nA_v(b-2c)}{s(b-2c)(h-2c)} + \frac{2A_v b}{sbh};\qquad \rho_y = \frac{nA_v(h-2c)}{s(b-2c)(h-2c)} + \frac{2A_v d_1}{sbh} \tag{14}$$

where $Ø_{sc}$ = the diameter of external steel-rod collars.

Then the compressive strength of concrete (f'_{cc}), strain at the compressive strength (ε'_{cc}), crushing strength (f'_{cu}), strain at crushing strength (ε'_{cu}) were calculated according to the Mander et al. model and assigned to the Concrete02 material model in OpenSees. The residual stress in the descending branch is considered as 20 % of f'_{cc}. Table 2 summarizes the properties used in the model.

DOI:10.4186/ej.2020.24.3.107

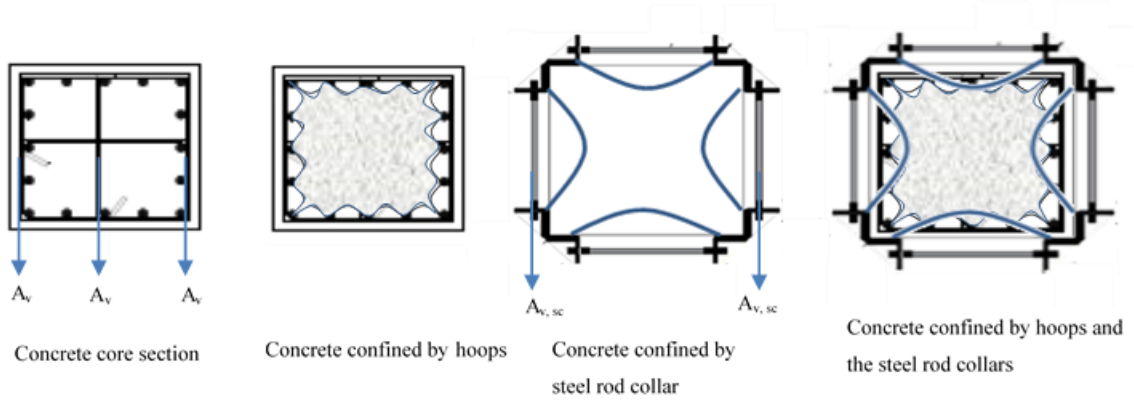

Fig. 27. Models for identifying concrete confined by hoops and the steel rod collars.

Table 2. Concrete material properties.

Specimen	Materials	f_c' (MPa)	ε_{cc}'	f_{cu}' (MPa)	ε_{cu}'
CC	Unconfined Concrete	31.5	0.002	0	0.0046
	Confined Concrete	32.7	0.0024	6.6	0.0086
SC-200	Unconfined Concrete	31.5	0.002	0	0.0046
	Confined Concrete	35.4	0.0032	7.1	0.0180
SC -100	Unconfined Concrete	31.5	0.002	0	0.0046
	Confined Concrete	37.9	0.004	7.6	0.0270

5.2.3. Reinforcing steel

The Giuffre-Menegotto-Pinto model was used for the Steel02 material model in OpenSees. For the steel material model in OpenSees, yield strength of longitudinal steel (f_y), initial elastic tangent (E_0), strain hardening ratio (B_s), parameters to control the transition from elastic to plastic branches (R_0, CR1, CR2) are required. Key material properties are presented in Table 3.

Table 3. Steel material properties.

f_y (MPa)	E_s (MPa)	B_s	R_0	CR1	CR2
515	200000	0.01	18	0.925	0.15

5.2.4. Rotational slip spring

The elastic rotational stiffness, which was originally suggested by Elwood and Eberhard, 2009 [28] was determined using the following expression:

$$K_{slip} = \frac{8\mu M_y}{d_b f_y \emptyset_y} \quad (15)$$

where d_b = nominal diameter of vertical steel bars; M_y = yielding moment; $\emptyset_y$ = yielding curvature; μ = the uniform bond stress along the embedded length.

The value of the uniform bond stress proposed by Elwood and Eberhard, 2009 [28] was considered as $0.8\sqrt{f_c'}$ MPa. The yield moment and yield curvature were obtained from the moment curvature analysis of the column section.

5.2.5. Shear spring

The non-linear behavior of the control column was modelled using the shear spring element. The spring element was created using a zero-length element in OpenSees. In order to accurately describe the shear limit curve, it is very essential to define descending slope (K_{deg}) shown in Fig. 28.

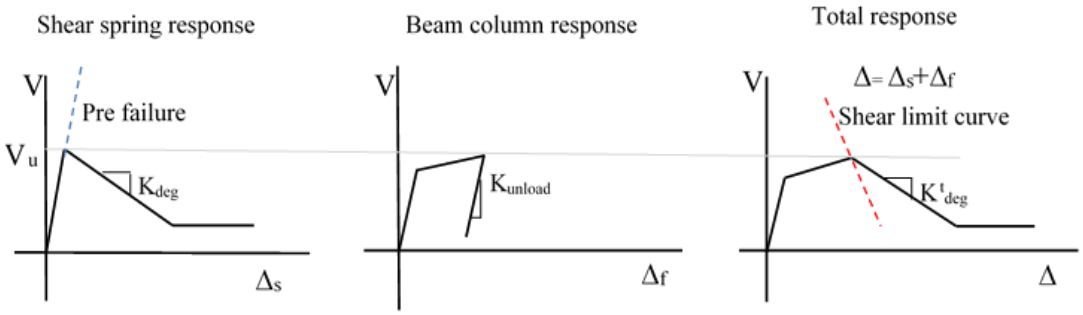

Fig. 28. Concept of shear limit response.

When the shear failure occurs, K^t_{deg} can be calculated based on the intersection of the shear limit curve and total response as follows:

$$K^t_{deg} = \frac{V_u}{\Delta_a - \Delta_s} \tag{16}$$

where V_u = ultimate capacity; Δ_s = displacement corresponding to shear failure; Δ_a = displacement corresponding to axial failure.

In this study, no axial failure occurred in the control column. Therefore, the displacement at the axial failure was neglected. The displacement at shear failure was determined using the model proposed by Elwood and Eberhard, 2009 [28].

$$\frac{\Delta_s}{L} = \frac{3}{100} + 4\rho_v - \frac{1}{40}\frac{\nu}{\sqrt{f_c'}} - \frac{1}{40}\frac{P}{A_g f_c'} \geq \frac{1}{100}\ (\text{MPa}) \tag{17}$$

where $\frac{\Delta_s}{L}$ = drift ratio at shear failure; ρ_v = ratio of transverse steel bars; ν = nominal shear stress.

The total flexibility can be considered as the sum of the shear spring and beam element flexibilities because both shear spring and beam element are in series. Therefore, K_{deg} can be determined by using following expression:

$$K_{deg} = \left(\frac{1}{K^t_{deg}} - \frac{1}{K_{unload}} \right)^{-1} \tag{18}$$

where K_{unload} = unloading stiffness of beam element.

In this study, K_{unload} is calculated using following expression:

$$K_{unload} = \frac{3EI_{eff}}{L^3} \tag{19}$$

where EI_{eff} = effective flexural stiffness; L = length of RC column.

5.3. Results and Discussions

The analytical results are compared with test results as shown in Figs. 29-31 for the columns CC, SC-200, and SC-100, respectively. It can be noticed that the behavior of the shear-dominated column (control specimen CC) can be captured well by the model with the rotational slip spring and the shear spring. The strength degradation after the peak load of the model agrees well with the test result. For the strengthened specimens which fail in the flexural mode, the load-displacement relation from the analysis matches satisfactorily with that from the experiment. The fiber model with the proposed method to determine the confinement effect can well represent the actual behavior of the columns strengthened by the steel-rod collars. The confinement from the column ties and the steel-rod collars should be combined to take into account the enhancement in confinement. Note that the hysteresis loops after the peak load, which is mainly governed by longitudinal steel reinforcement are different between the analysis and experiment. The improvement can be further investigated, one of which is the buckling model of the longitudinal reinforcement.

DOI:10.4186/ej.2020.24.3.107

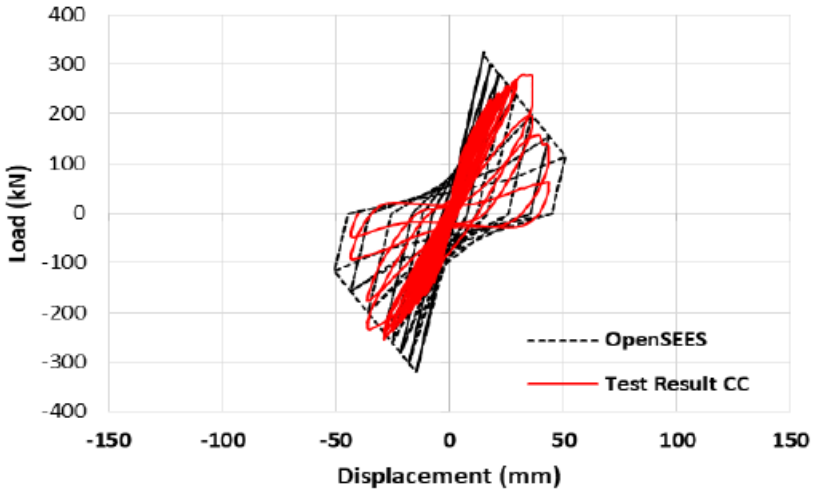

Fig. 29. Numerical results versus experimental results for the control column.

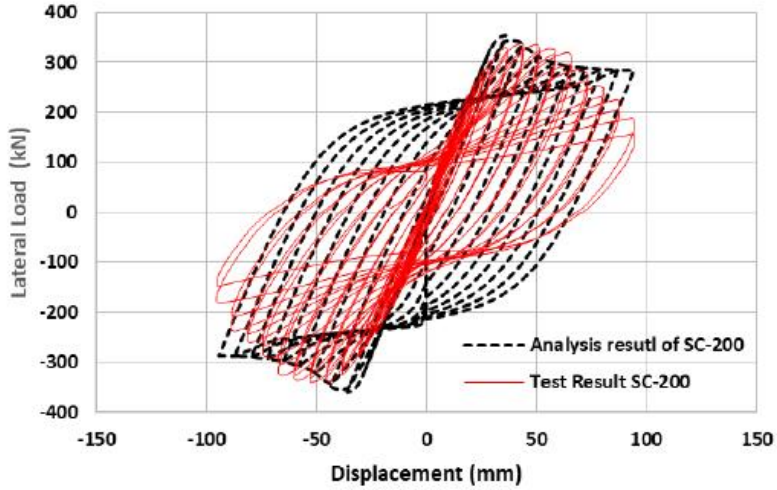

Fig. 30. Numerical results versus experimental results for column SC-200.

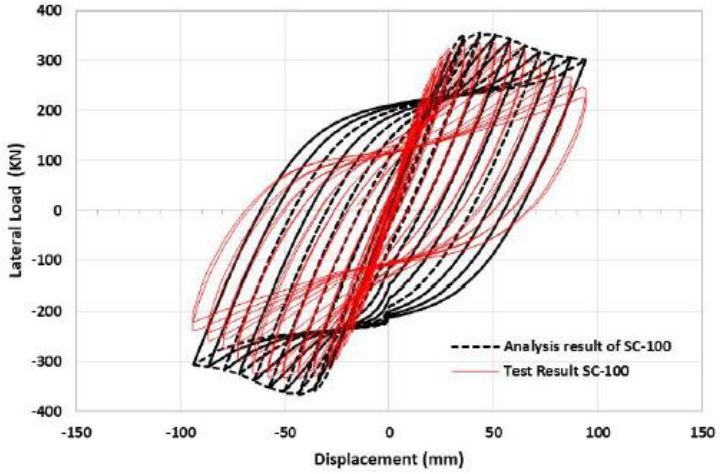

Fig. 31. Numerical results versus experimental results for column SC-100.

6. Conclusions

In this study, the effectiveness of high-strength steel-rod collars in the enhancement of shear critical columns was investigated by a series of experiment and analyses. Based on the study, following conclusions could be drawn:

(1) The test on the controlled shear critical column (Specimen CC) showed that the column experienced the premature shear failure after reaching the maximum load. Shear cracks developed rapidly during strength degradation. Both strengthened specimens i.e., SC-200 and SC-100 failed in flexure at the drift ratios larger than 5%, which were more than twice the lateral drift capacity of the controlled column. The increase in the lateral load capacity and ductility ratio of SC-200 was 18 % and 59% comparing with the control column, respectively. The increase in the lateral load capacity and ductility ratio of SC-100 was 16% and 69% comparing with the controlled column, respectively. The strengthened specimens had the stable hysteretic behaviors, higher ductility factors and higher energy dissipation than the un-strengthened RC column.

(2) The steel-rod collars helped reduce the strains in the transverse steels in the columns as the shear force was carried by the steel-rod collars as indicated by the strains measured in the steel-rod collars. The strains in the steel-rod collars were lower than the yield strain.

(3) The numerical analysis of the shear critical column (Specimen CC) shows that its behavior can be captured well by the analytical model with the rotational slip spring and the shear spring.

(4) The numerical analysis of strengthening columns was performed using the lumped plasticity fiber model. The load-displacement relations from the analysis are found close to the experimental results. In general, the analytical predictions of lateral loads are found slightly higher than the experimental results. The fiber model with the proposed method to determine the confinement effect can well represent the actual behavior of the columns strengthened by the steel-rod collars. The confinement from the column ties and the steel-rod collars should be combined in determining the confinement effects.

Acknowledgement

The authors appreciate the financial support from AUN/SEED-Net and The Thailand Research Fund (TRF) for this study.

References

[1] O. S. Kwon and E. Kim, "Case study: Analytical investigation on the failure of a two-story RC building damaged during the 2007 Pisco-Chincha earthquake," *Eng. Struct.*, vol. 32, no. 7, pp. 1876-87, 2010.

[2] C. Zhou, X. Lu, H. Li, and T. Tian, "Experimental study on seismic behavior of circular RC columns strengthened with pre-stressed FRP strips," *Earth. Eng. Eng. Vib.*, vol. 12, no. 4, pp. 625-42, 2013.

[3] M. Frangou, K. Pilakoutas, and S. Dritsos, "Structural repair/strengthening of RC columns," *Constr. Build. Mater.*, vol. 9, no. 5, pp. 259-66, 1995.

[4] I. Erdem, U. Akyuz, U. Ersoy, and G. Ozcebe, "An experimental study on two different strengthening techniques for RC frames," *Eng. Struct.,* vol. 28, no. 13, pp. 1843-51, 2006.

[5] K. G. Vandoros and S.E. Dritsos, "Concrete jacket construction detail effectiveness when strengthening RC columns," *Constr. Build. Mater.*, vol. 22, no. 3, pp. 264-76, 2008.

[6] E. N. Júlio and F. A. Branco, "Reinforced concrete jacketing-Interface influence on cyclic loading response," *ACI Struct. J.*, vol. 105, no. 4, pp. 471, 2008.

[7] M. Rodriguez and R. Park, "Seismic load tests on reinforced concrete columns strengthened by jacketing," *Struct. J.*, vol. 91, no. 2, pp. 150-159, 1994.

[8] S. N. Bousias, D. Biskinis, M. N. Fardis, and A. L. Spathis, "Strength, stiffness, and cyclic deformation capacity of concrete jacketed members," *ACI Struct. J.*, vol. 104, no. 5, pp. 521, 2007.

[9] J. Ramírez, "Ten concrete column repair methods," *Constr. Build. Mater.*, vol. 10, no. 3, pp. 195-202, 1996.

[10] Y. Xiao and H. Wu, "Retrofit of reinforced concrete columns using partially stiffened steel jackets," *J. Struct. Eng.*, vol. 129, pp. 725-732, 2003.

[11] E. Choi, J. Park, T.-H. Nam, and S.-J. Yoon, "A new steel jacketing method for RC columns," *Mag. Concrete Res.*, vol. 61, pp. 787-796, 2009.

[12] R. S. Aboutaha, M. D. Engelhardt, J. O. Jirsa, and M. E. Kreger, "Rehabilitation of shear critical concrete columns by use of rectangular steel jackets," *Struct. J.*, vol. 96, no. 1, pp. 68-78, 1999.

[13] Y. H Chai, M. N. Priestley, and F. Seible, "Analytical model for steel-jacketed RC circular bridge columns," *J. Struct. Eng.*, vol. 120, no. 8, pp. 2358-2376, 1994.

[14] A. M. Tarabia and H. F. Albakry, "Strengthening of RC columns by steel angles and strips," *Alexandria Eng. J.*, vol. 53, no. 3, pp. 615-626, 2014.

[15] D. I. McLean and L. L. Bernards, "Seismic retrofitting of rectangular bridge column for shear," Washington State Department of Transportation, WA, 1992.

[16] American Concrete Institute, "318-14 Building code requirements for structural concrete and commentary," MI, 2014.

[17] ASTM International, ASTM C39/C39M Standard test method for compressive strength of cylindrical concrete specimens, PA, 2020.

[18] ASTM International, ASTM E8/E8M Standard test method for tensile testing of metallic materials, PA, 2013.

[19] H. Sezen and J. P. Moehle, "Shear strength model for lightly reinforced concrete columns," *J. Struct. Eng.*, vol. 130, no. 11, pp. 1692-1703, 2004.
[20] J. B. Mander, M. J. Priestley, and R. Park, "Theoretical stress-strain model for confined concrete," *J. Struct. Eng.*, vol. 114, no. 8, pp. 1804-1826, 1988.
[21] S. Mazzoni, F. McKenna, M. H. Scott, and G. L. Fenves, "OpenSees command language manual," Pacific Earthquake Engineering Research Center, University of California, Berkeley, CA, 2009.
[22] X. Huang and O. S. Kwon, "Numerical models of RC elements and their impacts on seismic performance assessment," *Earth. Eng. Struct. Dynam.*, vol. 44, no. 2, pp. 283-298, 2015.
[23] X. Huang, "Applicability criteria of fiber-section elements for the modelling of RC columns subjected to cyclic loading," M.Eng. Thesis, University of Toronto, 2012.
[24] M. H. Scott and G. L. Fenves, "Plastic hinge integration methods for force-based beam–column elements," *J. Struct. Eng.*, vol. 132, no. 2, pp. 244-252, 2006.
[25] D. C. Kent and R. Park, "Flexural members with confined concrete," *J. Struct. Div.*, 1971.
[26] R. Montuori and V. Piluso, "Reinforced concrete columns strengthened with angles and battens subjected to eccentric load," *Eng. Struct.*, vol. 31, no. 2, pp. 539-550, 2009.
[27] G. Campione, L. Cavaleri, F. Di. Trapani, and M. F. Ferrotto, "Frictional effects in structural behavior of no-end-connected steel-jacketed RC columns: Experimental results and new approaches to model numerical and analytical response," *J. Struct. Eng.*, vol. 143, no. 8, 2017.
[28] K. J. Elwood and M. O. Eberhard, "Effective stiffness of reinforced concrete columns," *ACI Struct. J.*, vol. 106, no. 4, 2009.

Phawe Suit Theint, photograph and biography not available at the time of publication.

Anat Ruangrassamee, photograph and biography not available at the time of publication.

Qudeer Hussain, photograph and biography not available at the time of publication.